MATHEMATICAL BIOSCIENCES
AND ENGINEERING
Volume **13**, Number **2**, April **2016**

doi:10.3934/mbe.2015010

pp. **425–442**

MODELING THE INTRINSIC DYNAMICS OF FOOT-AND-MOUTH DISEASE

Steady Mushayabasa

Department of Mathematics, University of Zimbabwe
P.O. Box MP 167, Harare, Zimbabwe

Drew Posny

NSF Center for Integrated Pest Management, NC State University
Raleigh, NC 27606, USA
and
USDA, ARS, US Horticultural Research Laboratory
Fort Pierce, FL 34945, USA

Jin Wang*

Department of Mathematics, University of Tennessee at Chattanooga
Chattanooga, TN 37403, USA

(Communicated by Jia Li)

Abstract. We propose a new mathematical modeling framework to investigate the transmission and spread of foot-and-mouth disease. Our models incorporate relevant biological and ecological factors, vaccination effects, and seasonal impacts during the complex interaction among susceptible, vaccinated, exposed, infected, carrier, and recovered animals. We conduct both epidemic and endemic analysis, with a focus on the threshold dynamics characterized by the basic reproduction numbers. In addition, numerical simulation results are presented to demonstrate the analytical findings.

1. **Introduction.** Foot-and-mouth disease (FMD) remains one of the most contagious transboundary animal disease affecting cloven hoofed animals [15, 16]. Infection with the disease, caused by the FMD virus (FMDV), is characterized by fever and vesicles in or around the mouth, the digits of the feet, and the teats or mammary glands. FMD is endemic in Zimbabwe and several other African countries and constitutes a significant constraint to international trade in live animals and animal products [20]. The disease can be controlled through vaccination of susceptible animals and treatment or culling of infectious animals. During the 2001 FMD outbreak in the United Kingdom (UK), it is estimated that more than 2000 farms with approximately six million animals were culled. Further, the total loss, composed of agriculture and food chain as well as compensation for slaughtered animals and clean-up costs, summed up to about 3.1 billion pounds and 2.5 billion pounds, respectively [7]. Thus, disease management and control are essential in order to minimize such risks as well as prevent large economical loss. Designing effective control measures entails the knowledge of the patterns of movements and contacts

2010 *Mathematics Subject Classification.* 92B05, 93A30, 93C15.
Key words and phrases. Foot-and-mouth disease, mathematical models, threshold dynamics.
* Corresponding author: Jin-Wang02@utc.edu.

and infection spread among the hosts, which define the fundamental transmission dynamics of the disease.

Since the 2001 UK outbreak, several mathematical models have been proposed to explore the FMD transmission dynamics (see [4, 5, 8–11, 19], to mention a few). Dekker et al. [5] investigated the rate of FMDV transmission by carriers using published experimental data. Kao et al. [8] introduced a static network-based framework for analyzing the epidemic spread and corroborated the results with a stochastic epidemic model. Keeling et al. [9] investigated the role of national prophylactic vaccination campaigns and culling strategies during an FMD outbreak. Their study revealed, among other findings, that in the presence of sufficient resources and adequate preparation, a combination of reactive vaccination and culling may effectively control FMD transmission. Recently, Ringa and Bauch (2014) [19] developed an SEIRVC (Susceptible-Exposed-Infectious-Recovered-Vaccinated-Culled) pair approximation model of FMD transmission in near-endemic populations. Their work suggested that optimal long-term control of FMD by vaccination in near-endemic settings can be achieved by rolling out prophylactic vaccine as much as possible, especially if resources are limited.

Despite these efforts in modeling and analyzing FMD dynamics, several important questions regarding the transmission and spread of the disease remain to be answered. For example, how to characterize the role of disease carriers in an FMD outbreak? How to measure the epidemic risk under disease control measures, particularly vaccination? And how does the interaction between infected animals and others (susceptible, vaccinated, carriers, etc.) shape the short- and long-term dynamics of FMD? In addition, like many other infectious diseases, FMD is significantly impacted by environmental and climatic factors. Particularly, seasonal variation causes periodic changes in pastures and the movement and contact patterns of animals, which results in disease dynamics not captured by mathematical models with constant parameters. Currently, very little work has been devoted to investigating FMD dynamics under seasonal impact.

In this paper, we propose a mathematical framework to study the intrinsic dynamics of FMD, incorporating relevant biological details, vaccination effects, and seasonal oscillation. We will start with a basic compartment model represented by an autonomous ODE system that depicts the interaction among susceptible, vaccinated, exposed, infected, carrier, and recovered animals. We conduct epidemic and endemic analysis and investigate disease threshold dynamics characterized by the basic reproduction number. We then proceed to study FMD dynamics under seasonal impact, by computing the basic reproduction number for the periodic model and establishing it as a sharp threshold for disease dynamics in periodic environments. In addition, numerical results are presented to demonstrate the analytic prediction, and conclusions are drawn in the end of the paper.

2. **Mathematical modeling, analysis and results.**

2.1. **Basic model.**

Let $S(t)$, $H(t)$, $E(t)$, $I(t)$, $C(t)$ and $R(t)$ represent the proportion of susceptible, vaccinated, exposed, infected, carrier and recovered animals at time t, respectively, with a (normalized) total population $N(t) = S(t) + H(t) + E(t) + I(t) + C(t) + R(t)$. FMD dynamics in this study are governed by the following nonlinear system:

$$\begin{cases} \dot{S}(t) &= \mu - \lambda S(t) - (\mu+\phi)S(t) + \alpha H(t), \\ \dot{H}(t) &= \phi S(t) - (1-\epsilon)\lambda H(t) - (\mu+\alpha)H(t), \\ \dot{E}(t) &= \lambda(S(t) + (1-\epsilon)H(t)) - (\mu+\gamma)E(t), \\ \dot{I}(t) &= (1-\kappa)\gamma E(t) - (\mu+\sigma)I(t), \\ \dot{C}(t) &= \kappa\gamma E(t) + \sigma\pi_0 I(t) - (\mu+d)C(t), \\ \dot{R}(t) &= \sigma\pi_2 I(t) + (1-p)dC(t) - \mu R(t). \end{cases} \tag{1}$$

Figure 1 illustrates the model flow chart for the system.

The constant parameter μ denotes the constant rate of entry for new animals into the susceptible class. We assume that it also equals the non-FMD related exit rate and is assumed to be the same for all classes. Susceptible animals are vaccinated at rate ϕ, while vaccinated animals lose vaccine-induced immunity at constant rate α. The average period of natural and vaccine protection depends on a number of factors such as the virus serotype, affected species, and the type of vaccine administered. Prior studies estimate this period to range from 6 months to 5.5 years [19]. Susceptible animals are exposed to FMD through direct contact with infectious animals, with a bilinear incidence representation

$$\lambda = \beta I\,,$$

where β denotes the disease transmission rate. Meanwhile, vaccinated animals are assumed to acquire FMD at a reduced rate modeled by $(1-\epsilon)\beta I$. Here, $(1-\epsilon)$ represents the vaccine protective factor, and ϵ represents the vaccine efficacy which depends on the type of vaccine used. In a recent study conducted by Knight-Jones et al. [12], it was observed that FMD vaccination can be 89% effective to protect susceptible animals against FMDV.

FMD exposed animals remain in the exposed state for γ^{-1} days on average (incubation) after which a fraction $(1-\kappa)$ become infected and the complementary fraction κ become FMD carriers. The incubation period for FMD can vary depending on the species of the infected animal, the dose of the virus, the viral strain and the route of inoculation [1]. In particular, for cattle population, the reported incubation period ranges between 2-14 days [15, 19]. Prior studies suggest that animals can become FMD carriers whether or not they had clinical signs [1]. Although there are anecdotal reports of apparent transmission from these animals in the field, and esophageal-pharyngeal fluid is infectious if it is injected directly into an animal, all attempts to demonstrate transmission between domesticated livestock in close contact during controlled experiments have failed [1].

Further, the proportion of exposed and infected cattle which become carriers is estimated to range from 15-50% [2]. Infected animals remain in this state for σ^{-1} days. Depending on the FMDV strain and the animal species, infected animals remain symptomatic of FMD and infectious for about 7 -10 days before they either become carriers, succumb to FMD-induced death, or recover [19]. Model parameters π_0, π_1 and π_2 denote the proportions of infected animals which progress to the carrier population, suffer FMD-related mortality, and successfully recover from infection, respectively. Thus, $\pi_0 + \pi_1 + \pi_2 = 1$. FMD-related mortality, though generally low, varies with species, age of the animal, breed, and pre-existing immunity

as well as the dose of the virus and a host of other factors. In adult live stock, the fatality is estimated to be between 0-5% [1]. Carrier animals remain in the carrier state for d^{-1} days. Prior studies suggest that cattle can be in the carrier state for a period as long as 3.5 years [1,2]. We may assume that a fraction p of carrier animals succumb to FMD-related death and the remainder $(1-p)$ successfully recover from the disease.

In Table 1, we present the values for the model parameters.

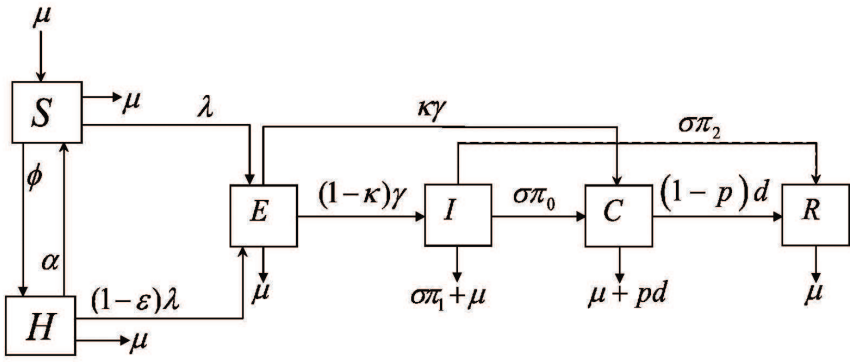

FIGURE 1. Model flowchart

Parameter Definition	Symbol	Baseline value	Units	Source
Exit rate	μ	0.001	day^{-1}	[13]
Vaccination rate	ϕ	0.006	day^{-1}	[19]
Incubation period	γ^{-1}	4	days	[15, 19]
Vaccine waning rate	α	0.0056	day^{-1}	[19]
Average carrier period	d^{-1}	3.5	years	[1, 2]
FMD transmission rate	β	0.6	day^{-1}	[19]
Average infectious period	σ^{-1}	7	days	[19]
Vaccine efficacy	ϵ	0.89 (0.5-0.89)	-	[12]
Proportion of infectious animals which progress to carrier population	π_0	0.35 (0.15-0.5)	-	[1, 2]
Proportion of infectious animals which succumb to FMD-induced death	π_1	0 (0.0-0.05)	-	[1]
Proportion of infectious animals which recover from FMD	π_2	0.65 (0.45-0.85)	-	[1, 2]
Proportion of exposed animals which become FMD carriers	κ	0.5 (0.15-0.5)	-	[2]
Proportion of FMD carriers which succumb to disease related death	p	0 (0.0-0.05)	-	[1]

TABLE 1. Model parameters and their interpretations.

It can be easily verified that all solutions of the system (1) with non-negative initial conditions remain positive. Moreover, considering that the death rates for the infected and carrier animals, π_1 and p respectively, are typically very low [1,2], in what follows we will assume that $\pi_1 = p = 0$. With this assumption, we can easily

observe from the system (1) that $N(t) = S(t)+H(t)+E(t)+I(t)+C(t)+R(t) = 1$ for all t. Meanwhile, consider the first equation from system (1). Since $S(t)+H(t) \leq 1$, it follows that

$$\frac{dS}{dt} \leq \mu - (\mu+\phi)S(t) + \alpha H(t) \leq (\mu+\alpha) - (\mu+\phi+\alpha)S(t). \tag{2}$$

Thus,

$$S(t) \leq \frac{\mu+\alpha}{\mu+\phi+\alpha} \triangleq S^0 \tag{3}$$

provided that $S(0) \leq S^0$. Similarly, from the second equation of system (1) we obtain

$$\frac{dH}{dt} \leq \phi S(t) - (\mu+\alpha)H(t) \leq \phi - (\mu+\alpha+\phi)H(t). \tag{4}$$

Thus,

$$H(t) \leq \frac{\phi}{\mu+\alpha+\phi} \triangleq H^0 \tag{5}$$

as long as $H(0) \leq H^0$. We conclude that the feasible region

$$\Omega = \left\{(S,H,E,I,C,R) \in [0,1]^6 : S \leq S^0, H \leq H^0, S+H+E+I+C+R = 1\right\} \tag{6}$$

is positively invariant with respect to the system (1).

2.2. **The reproductive number.** In the absence of FMDV in the community, system (1) exhibits an equilibrium point known as the FMD-free (denoted by $\mathcal{E}_0$):

$$\mathcal{E}^0 = \left(S^0, H^0, E^0, I^0, C^0, R^0\right) = \left(\frac{\alpha+\mu}{\alpha+\mu+\phi}, \frac{\phi}{\alpha+\mu+\phi}, 0, 0, 0, 0\right). \tag{7}$$

In infectious disease modeling, the basic reproductive number often denoted as $\mathcal{R}_0$ plays a crucial role on exploring the power of the disease to invade the population. The basic reproduction number is defined as the average number of secondary cases caused by a typical infected animal throughout its entire course of infection in a completely susceptible population and in the absence of control interventions [6]. In the context of a partially susceptible population owing to prior exposure or vaccination, the basic (or, effective) reproduction number quantifies the potential risk for infectious disease transmission. If the effective reproductive number is less than or equal to unity, then transmission chains are not self-sustaining and are unable to generate a major epidemic. By contrast, an epidemic is likely to occur whenever the effective reproductive number is greater than unity.

Using the next generation matrix approach outlined in [21], the effective reproductive number $\mathcal{R}_e$ of system (1) can be found as

$$\mathcal{R}_e = \frac{\beta\gamma(1-\kappa)(\alpha+\mu+(1-\epsilon)\phi)}{(\mu+\gamma)(\mu+\sigma)(\mu+\alpha+\phi)}. \tag{8}$$

Clearly, $\mathcal{R}_e$ depends on several model parameters, particularly the FMD transmission rate, β, and the vaccination protective factor, ϵ. A contour plot of $\mathcal{R}_e$ as a function of β and ϵ is presented in Figure 2. The values of other model parameters are based on Table 1. We observe that when β becomes larger or when ϵ is reduced, $\mathcal{R}_e$ increases, implying a higher disease risk. In particular, when the transmission rate is sufficiently high (> 0.45 per day), the value of $\mathcal{R}_e$ is always higher than 1 regardless of the efficacy of the vaccination, an indication that FMD would persist in the community. In what follows we mathematically justify these observations

and establish $\mathcal{R}_e = 1$ as a sharp threshold for the disease dynamics of the model (1).

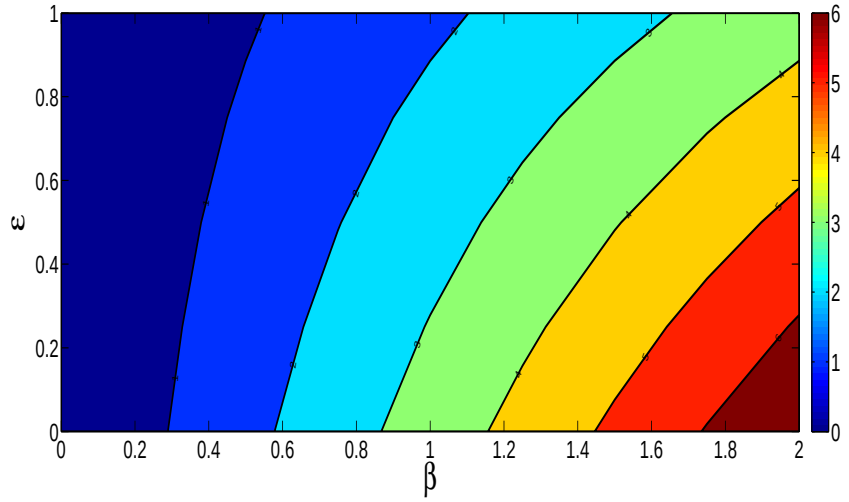

FIGURE 2. Contour plot of $\mathcal{R}_e$ as a function of β (FMD transmission rate) and ϵ (FMD vaccine protective factor). Other parameters are fixed and their values are provided in Table 1.

The local stability of the disease-free equilibrium $\mathcal{E}^0$ when $\mathcal{R}_e < 1$, and the instability of $\mathcal{E}^0$ when $\mathcal{R}_e > 1$, can be directly obtained from the standard result in [21]. We now claim the following result.

Theorem 2.1. *When $\mathcal{R}_e \leq 1$, the FMD-free equilibrium $\mathcal{E}^0$ is globally asymptotically stable in Ω.*

Proof. Consider the following Lyapunov function

$$L(t) = \frac{\beta\gamma(1-\kappa)}{(\mu+\gamma)(\mu+\sigma)}E(t) + \frac{\beta}{(\mu+\sigma)}I(t)\,.$$

Differentiating L along the solutions of the system (1) yields

$$\begin{aligned}
\frac{dL}{dt} &= \frac{\beta\gamma(1-\kappa)}{(\mu+\gamma)(\mu+\sigma)}\frac{dE}{dt} + \frac{\beta}{(\mu+\sigma)}\frac{dI}{dt} \\
&= \beta\left[\frac{\beta\gamma(1-\kappa)[S+(1-\epsilon)H]}{(\mu+\gamma)(\mu+\sigma)} - 1\right] I(t) \\
&\leq \beta\left[\frac{\beta\gamma(1-\kappa)(\alpha+\mu+(1-\epsilon)\phi)}{(\mu+\gamma)(\mu+\sigma)(\mu+\alpha+\phi)} - 1\right] I(t) \\
&= -\beta(1-\mathcal{R}_e)I(t).
\end{aligned} \tag{9}$$

Thus, $\dot{L} \leq 0$ as long as $\mathcal{R}_e \leq 1$. When $\mathcal{R}_e < 1$, $\dot{L} = 0$ yields $I = 0$. Then it can be easily observed from the system (1) that as $t \to \infty$, $E \to 0, C \to 0, R \to 0$, and $S \to S^0$, $H \to H^0$. Hence, the only invariant set when $\dot{L} = 0$ is the singleton

$\mathcal{E}^0 = (S^0, H^0, 0, 0, 0, 0)$. It follows from Lasalle's Invariance Principle [14] that every solution of the system (1), with initial conditions in Ω, approaches $\mathcal{E}^0$ as $t \to \infty$.

When $\mathcal{R}_e = 1$, $\dot{L} = 0$ implies either $I = 0$, or

$$1 = \frac{\beta\gamma(1-\kappa)[S + (1-\epsilon)H]}{(\mu+\gamma)(\mu+\sigma)} \leq \frac{\beta\gamma(1-\kappa)(\alpha+\mu+(1-\epsilon)\phi)}{(\mu+\gamma)(\mu+\sigma)(\mu+\alpha+\phi)} = \mathcal{R}_e = 1.$$

The latter case yields $S = S^0 = \frac{\alpha+\mu}{\alpha+\mu+\phi}$ and $H = H^0 = \frac{\phi}{\alpha+\mu+\phi}$ and, consequently, $E = I = C = R = 0$. Hence, in either case, the only invariant set for $\dot{L} = 0$ is the singleton $\mathcal{E}^0 = (S^0, H^0, 0, 0, 0, 0)$, and the conclusion again follows from LaSalle's Invariance Principle. □

2.3. **Endemic equilibrium.** In order to investigate the long-term dynamics of FMD, we conduct an endemic analysis when $\mathcal{R}_e > 1$. The following theorem shows the existence and uniqueness of the endemic equilibrium.

Theorem 2.2. *When $\mathcal{R}_e > 1$, there exists a unique endemic equilibrium of the system (1).*

Proof. Let us denote the endemic equilibrium of the system (1) by $\mathcal{E}^* = (S^*, H^*, E^*, I^*, C^*, R^*)$, where

$$\begin{aligned}
S^* &= \frac{\mu\left((1-\epsilon)\beta I^* + (\mu+\alpha)\right)}{[\beta I^* + (\mu+\phi)][(1-\epsilon)\beta I^* + (\mu+\alpha)] - \alpha\phi} \\
H^* &= \frac{\phi\mu}{[\beta I^* + (\mu+\phi)][(1-\epsilon)\beta I^* + (\mu+\alpha)] - \alpha\phi} \\
I^* &= \left(\frac{(\mu+\gamma)(\mu+\sigma)}{(1-\kappa)\gamma\beta[S^* + (1-\epsilon)H^*]}\right) I^* \\
E^* &= \frac{(\mu+\sigma)}{(1-\kappa)\gamma} I^* \\
C^* &= \frac{1}{\mu+d}\left[\frac{\kappa(\mu+\sigma)}{1-\kappa} + \sigma\pi_0\right] I^* \\
R^* &= \frac{1}{\mu}\left[\sigma\pi_2 + \frac{(1-\rho)d}{\mu+d}\left(\frac{\kappa(\mu+\sigma)}{1-\kappa} + \sigma\pi_0\right)\right] I^*
\end{aligned}$$

It is easily observed that C, R and E are constant multiples of I. Furthermore, we may treat S and H as implicit functions of I, and let

$$g(I) = S(I) + (1-\epsilon)H(I)\,, \quad g_1(I) = \beta I + (\mu+\phi)\,, \quad \text{and} \quad g_2(I) = (1-\epsilon)\beta I + (\mu+\alpha).$$

Therefore, we have that at an equilibrium,

$$S(I) = \frac{\mu g_2(I)}{g_1(I)g_2(I) - \alpha\phi}\,, \qquad H(I) = \frac{\phi\mu}{g_1(I)g_2(I) - \alpha\phi}\,, \tag{10}$$

and

$$I = \left(\frac{(\mu+\gamma)(\mu+\sigma)}{(1-\kappa)\gamma\beta g(I)}\right) I\,. \tag{11}$$

From equation (11) and $I \neq 0$, it follows that for an endemic equilibrium to exist we must have,

$$\frac{(\mu+\gamma)(\mu+\sigma)}{(1-\kappa)\gamma\beta} = g(I) \tag{12}$$

for some $I = I^* > 0$.

Clearly, g is differentiable for all $I \geq 0$. Taking the derivative of g yields the following

$$\begin{aligned} g'(I) &= S'(I) + (1-\epsilon)H'(I) \\ &= -\left(\frac{\mu[\alpha\phi + g_1'(I)(g_2(I))^2]}{[g_1(I)g_2(I) - \alpha\phi]^2} + (1-\epsilon)\frac{\phi\mu[g_1'(I)g_2(I) + g_1(I)g_2'(I)]}{[g_1(I)g_2(I) - \alpha\phi]^2} \right). \end{aligned}$$

For $I \geq 0$, it is obvious that $g_1(I) > 0$ and $g_2(I) > 0$, as well as $g_1'(I) > 0$ and $g_2'(I) > 0$. Thus, $g'(I) < 0$, implying that $g(I)$ is a decreasing curve on $[0, \infty]$.

To determine if the function $g(I)$ intersects the constant function from the lefthand side of equation (12), we must investigate $g(0)$. We have that $g(0) = S(0) + (1-\epsilon)H(0) = \frac{\alpha+\mu+(1-\epsilon)\phi}{\alpha+\mu+\phi}$. Using equation (8), we can easily observe that if $\mathcal{R}_e > 1$, then $g(I) > \frac{(\mu+\gamma)(\mu+\sigma)}{(1-\kappa)\gamma\beta}$, and there is a unique endemic equilibrium $I = I^*$; however, if $\mathcal{R}_e \leq 1$, then $g(I) \leq \frac{(\mu+\gamma)(\mu+\sigma)}{(1-\kappa)\gamma\beta}$, and there is no endemic equilibrium. □

In order to investigate the local stability of the endemic equilibrium $\mathcal{E}^*$, we will make use of Theorem 3.1 (see the Appendix) based on the center manifold theory [3].

The Jacobian matrix of system (1) evaluated about the FMD-free equilibrium (7) is

$$J(\mathcal{E}^0) = \begin{pmatrix} -(\mu+\phi) & \alpha & 0 & -\frac{\beta(\alpha+\mu)}{\alpha+\mu+\phi} & 0 & 0 \\ \phi & -(\alpha+\mu) & 0 & \frac{\beta(1-\epsilon)\phi}{\alpha+\mu+\phi} & 0 & 0 \\ 0 & -(\mu+\gamma) & \frac{\beta(\alpha+\mu+(1-\epsilon)\phi}{\alpha+\mu+\phi} & 0 & 0 & \\ 0 & 0 & \kappa\gamma & \sigma\pi_0 & -(\mu+d) & 0 \\ 0 & 0 & 0 & \sigma\pi_2 & (1-p)d & -\mu \end{pmatrix}. \quad (13)$$

From (13), we can deduce that the left and right eigenvectors of system (1) are the following:

$$\begin{cases} w_1 &= -\dfrac{\beta(1-\kappa)\gamma[\alpha\phi(1-\epsilon) + (\alpha+\mu)^2]w_3}{\mu(\mu+\sigma)(\mu+\alpha+\phi)^2}, \\ w_2 &= -\dfrac{\beta(1-\kappa)\gamma\phi[\alpha+\mu+(1-\epsilon)(\mu+\phi)]w_3}{\mu(\mu+\sigma)(\mu+\alpha+\phi)^2}, \ w_3 > 0, \\ w_4 &= \dfrac{(1-\kappa)\gamma w_3}{\mu+\sigma}, \ w_5 = \left[\kappa\gamma + \dfrac{\sigma\pi_0(1-\kappa)\gamma}{\mu+\sigma}\right]\dfrac{w_3}{(\mu+d)}, \\ w_6 &= \left[\dfrac{\sigma(1-\kappa)\gamma}{\mu+\sigma}\left(\pi_2 + \dfrac{(1-p)\pi_0 d}{\mu+d}\right) + \dfrac{(1-p)\kappa\gamma d}{\mu+d}\right]\dfrac{w_3}{\mu}, \end{cases} \quad (14)$$

and

$$\begin{cases} v_1 &= v_2 = 0, \ v_3 > 0, \\ v_4 &= \dfrac{\beta[\mu+\alpha+(1-\epsilon)\phi]v_3}{(\mu+\sigma)(\mu+\phi+\alpha)}, \\ v_5 &= v_6 = 0. \end{cases} \quad (15)$$

Choosing model parameter β as the bifurcation parameter and solving $\mathcal{R}_e = 1$ gives

$$\beta = \frac{(\mu+\gamma)(\mu+\sigma)(\mu+\alpha+\phi)}{\gamma(1-\kappa)(\alpha+\mu+(1-\epsilon)\phi}. \tag{16}$$

Further, it can easily be verified that the bifurcation coefficients a and b, described in Theorem 3.1, are

$$\begin{aligned} a &= -\frac{\beta^2(1-\kappa)^2\gamma^2}{(\mu+\sigma)^2}\left[\frac{[\alpha\phi(1-\epsilon)+(\alpha+\mu)^2]+\phi[\alpha+\mu+(1-\epsilon)(\mu+\phi)]}{\mu(\mu+\alpha+\phi)^2}\right] w_3 v_3, \\ b &= \frac{\beta(1-\kappa)\gamma[\alpha+\mu+(1-\epsilon)\phi]}{(\mu+\sigma)(\mu+\phi+\alpha)} \\ &= w_3 v_3(\mu+\gamma)\mathcal{R}_e. \end{aligned}$$

It is clear that $a < 0$ and $b > 0$. Thus, from Theorem 3.1 we can establish the following result.

Theorem 2.3. *There is a forward transcritical bifurcation at $\mathcal{R}_e = 1$, and the endemic equilibrium $\mathcal{E}^*$ is locally asymptotically stable whenever $\mathcal{R}_e > 1$ but close to unity.*

2.4. **FMD dynamics in periodic environments.** In this section we investigate the dynamics of FMD in periodic environments representing seasonal changes. FMDV is transmitted when a susceptible animal comes into contact with an infectious animal. It is worth noting that the movement of animals from one area to another (searching for grazing pastures) heavily depends on seasonal variation, among other factors. We hypothesize that the seasonal movement and daily grazing activities of the mobile pastoralists have significant impacts on FMD transmission. Thus, we extend system (1) to incorporate seasonal effects on FMD dynamics.

For illustration, let us consider the time variation of the FMD transmission rate, one of the key model parameters. We define

$$\beta(t) = \beta_0\left[1 + a\sin\left(\frac{2\pi}{365}t + \varphi\right)\right], \tag{17}$$

where β_0 is the baseline value or the time average of $\beta(t)$, and a and φ denote the (relative) amplitude and phase, respectively, of the seasonal oscillation in $\beta(t)$. The function $\beta(t)$ has a period of $\omega = 365$ days, or 1 year. To ensure the positivity of $\beta(t)$, we require $0 < a < 1$. The new system describing FMD dynamics with seasonal variation is given by

$$\begin{cases} \dot{S}(t) &= \mu - \beta(t)I(t)S(t) - (\mu+\phi)S(t) + \alpha H(t), \\ \dot{H}(t) &= \phi S(t) - (1-\epsilon)\beta(t)I(t)H(t) - (\mu+\alpha)H(t), \\ \dot{E}(t) &= \beta(t)I(t)(S(t)+(1-\epsilon)H(t)) - (\mu+\gamma)E(t), \\ \dot{I}(t) &= (1-\kappa)\gamma E(t) - (\mu+\sigma)I(t), \\ \dot{C}(t) &= \kappa\gamma E(t) + \sigma\pi_0 I(t) - (\mu+d)C(t), \\ \dot{R}(t) &= \sigma\pi_2 I(t) + (1-p)dC(t) - \mu R(t) \end{cases} \tag{18}$$

As shown earlier in (6), it can be easily verified that system (18) has a unique and bounded solution with the initial value $(S_0, H_0, E_0, I_0, C_0, R_0) \in \Omega$, and that the compact set Ω is positively invariant with respect to system (18).

In what follows, we introduce the reproductive number of system (18) using the techniques presented in [17,22]. It is evident that system (18) has exactly one FMD-free equilibrium point $M_0 = \mathcal{E}^0$. Now, we introduce the next-generation matrices

$$F(t) = \begin{pmatrix} 0 & \dfrac{\beta(t)[\alpha+\mu+(1-\epsilon)\phi]}{\alpha+\mu+\phi} \\ 0 & 0 \end{pmatrix}, \text{ and } V(t) = \begin{pmatrix} (\mu+\gamma) & 0 \\ -(1-\kappa)\gamma & (\mu+\sigma) \end{pmatrix}.$$

In order to analyze the threshold dynamics of epidemiological models in periodic environments, Wang and Zhao [22] extended the framework in [21] by introducing the next infection operator

$$(L\phi)(t) = \int_0^\infty Y(t, t-s)F(t-s)\phi(t-s)ds\,, \tag{19}$$

where $Y(t,s)$, $t \geq s$, is the evolution operator of the linear ω-periodic system $\frac{dy}{dt} = -V(t)y$ and $\phi(t)$, the initial distribution of infectious animals, is ω-periodic and always positive. The effective reproductive number for a periodic model is then defined as the spectral radius of the next infection operator,

$$\mathcal{R}_0 = \rho(L). \tag{20}$$

The evolution operator $Y(t,s)$, for system (18) is

$$Y(t,s) = \begin{pmatrix} e^{-(\mu+\gamma)(t-s)} & 0 \\ \frac{(1-\kappa)\gamma}{\sigma-\gamma}\left[e^{-(\mu+\gamma)(t-s)} - e^{-(\mu+\sigma)(t-s)}\right] & e^{-(\mu+\sigma)(t-s)} \end{pmatrix}. \tag{21}$$

The next infection operator can be numerically evaluated by (see [17,18] for details)

$$(L\phi)(t) = \int_0^\infty Y(t, t-s)F(t-s)\phi(t-s)ds = \int_0^\omega G(t,s)\phi(t-s)ds,$$

where

$$\begin{aligned} G(t,s) &\approx \sum_{k=0}^{M} Y(t, t-s-k\omega)F(t-s-k\omega) \\ &\approx \frac{\alpha+\mu+(1-\epsilon)\phi}{\alpha+\mu+\phi}\,\beta(t-s)\sum_{k=0}^{M}\begin{bmatrix} 0 & e^{-(\mu+\gamma)(s+k\omega)} \\ 0 & \frac{(1-\kappa)\gamma}{\sigma-\gamma}\left[e^{-(\mu+\gamma)(s+k\omega)} - e^{-(\mu+\gamma)(s+k\omega)}\right] \end{bmatrix} \end{aligned} \tag{22}$$

Now we proceed to investigate the global stability of the FMD-free equilibrium for system (18), which will also provide a condition for the extinction of the disease.

Theorem 2.4. *If $\mathcal{R}_0 < 1$, the FMD-free equilibrium for system (18) is globally asymptotically stable in Ω.*

Proof. Consider the matrix function $F(t) - V(t)$:

$$F(t) - V(t) = \begin{pmatrix} -(\mu+\gamma) & \dfrac{\beta(t)[\alpha+\mu+(1-\epsilon)\phi]}{\alpha+\mu+\phi} \\ (1-\kappa)\gamma & -(\mu+\sigma) \end{pmatrix} \tag{23}$$

One can easily deduce that (23) is continuous, cooperative, irreducible and ω-periodic. Further, let $\Phi_{(F-V)(\cdot)}(t)$ be the fundamental solution matrix of the linear ordinary differential system:

$$\dot{x} = [F(t) - V(t)]x, \tag{24}$$

and $\rho(\Phi_{(F-V)(\cdot)}(\omega))$ be the spectral radius of $\Phi_{(F-V)(\cdot)}(\omega)$. Based on Lemma 2.1 in [22] we have the following result:

Lemma 1. *Let $\nu = (1/\omega)\ln\rho(\Phi_{(F-V)(\cdot)}(\omega)$. Then there exists a positive ω-periodic function $v(t)$ such that $e^{\nu t}v(t)$ is a solution to (24).*

With similar arguments as before, the first two equations of system (18) yield $S(t) \leq S^0$ and $H(t) \leq H^0$ in Ω. Next, we consider the third and fourth equations from the system (18), where it can now easily be seen that

$$\frac{d}{dt}\begin{bmatrix} E \\ I \end{bmatrix} \leq (F - V)\begin{bmatrix} E \\ I \end{bmatrix}. \tag{25}$$

From the aforementioned lemma, there exists $v(t)$ such that

$$x(t) = (\tilde{E}(t),\, \tilde{I}(t)) = e^{\nu t}v(t)$$

is a solution to equation (24), with $\nu = (1/\omega)\ln\rho(\Phi_{(F-V)(\cdot)}(\omega)$. Hence,

$$(E(t), I(t)) \leq (\tilde{E}(t), \tilde{I}(t))$$

when t is large, which would imply that

$$\lim_{t\to\infty} E(t) = 0 \qquad \text{and} \qquad \lim_{t\to\infty} I(t) = 0. \tag{26}$$

Consequently, from the fifth and sixth equations of system (18) it is straightforward to observe that

$$\lim_{t\to\infty} C(t) = 0 \tag{27}$$

and

$$\lim_{t\to\infty} R(t) = 0. \tag{28}$$

Meanwhile, we must return to the first two equations of the system (18). As $t \to \infty$, we have $I(t) \to 0$, thus by adding the first two equations together, we find that

$$\frac{d}{dt}(S + H) \to \mu - \mu(S + H)$$

which yields

$$S(t) + H(t) \to 1. \tag{29}$$

Hence,

$$\frac{dH}{dt} \to \phi(1 - H(t)) - (\mu + \alpha)H(t) = \phi - (\phi + \mu + \alpha)H(t),$$

or

$$H(t) \to \frac{\phi}{\phi + \mu + \alpha} = H^0, \tag{30}$$

which clearly leads to

$$S(t) \to 1 - H_0 = S^0. \tag{31}$$

Therefore,

$$\lim_{t\to\infty} x(t) = (S^0, H^0, 0, 0, 0, 0) \tag{32}$$

for all solutions $x(t)$. □

On the other hand, we study the dynamics of the system (18) when $\mathcal{R}_0 > 1$. We will show that when $\mathcal{R}_0 > 1$, the disease persists and there exists a positive periodic solution.

Theorem 2.5. *If $\mathcal{R}_0 > 1$, then the solutions of the system (18) are uniformly persistent, and the system admits at least one positive ω-periodic solution.*

Proof. Define

$$X = [0,1]^6; \quad X_0 = [0,1] \times [0,1] \times (0,1] \times (0,1] \times [0,1] \times [0,1]; \quad \partial X_0 = X \backslash X_0.$$

Clearly both X and X_0 are positively invariant with respect to the system. Let $P : X \to X$ be the Poincaré map associated with the system such that $P(x_0) = u(\omega, x_0)$ for all $x_0 \in X$, where $u(t, x_0)$ denotes the unique solution of the system with $u(0, x_0) = x_0$.

Set

$$M_\partial = \big\{ \big(S(0), H(0), E(0), I(0), C(0), R(0)\big) \in \partial X_0 : P^m\big(S(0), H(0), E(0), I(0), C(0), R(0)\big) \in \partial X_0, \ \forall m \geq 0 \big\}$$

and

$$\widetilde{M}_\partial = \big\{ \big(S, H, 0, 0, C, R\big) : 0 \leq S \leq 1, \ 0 \leq H \leq 1, \ 0 \leq C \leq 1, \ 0 \leq R \leq 1 \big\}.$$

We first show that

$$M_\partial = \widetilde{M}_\partial. \tag{33}$$

It is clear that $M_\partial \supseteq \widetilde{M}_\partial$. Meanwhile, consider any initial values $(S(0), H(0), E(0), I(0), C(0), R(0)) \in \partial X_0 \backslash \widetilde{M}_\partial$. If $E(0) = 0$ and $I(0) > 0$, then $E'(0) > 0$. Similarly, $I(0) = 0$ and $E(0) > 0$, then $I'(0) > 0$. It follows that $(S(t), H(t), E(t), I(t), C(t), R(t)) \notin \partial X_0$ for $0 < t \ll 1$. The positive invariance of X_0 implies that $M_\partial \subseteq \widetilde{M}_\partial$, and hence, equation (33) holds.

Now, consider the fixed point $M_0 = \big(\frac{\alpha+\mu}{\alpha+\mu+\phi}, \frac{\phi}{\alpha+\mu+\phi}, 0, 0, 0, 0\big)$ and define $W^S(M_0) = \{x_0 : P^m(x_0) \to M_0, m \to \infty\}$. From the system (18), it is easy to observe that when $E = I = 0$, we have $C(t) \to 0$, $R(t) \to 0$, and $S(t) \to S^0 = \frac{\alpha+\mu}{\alpha+\mu+\phi}$, $H(t) \to H^0 = \frac{\phi}{\alpha+\mu+\phi}$, as $t \to \infty$. Thus every orbit in $\widetilde{M}_\partial$ converges to M_0. We now prove that

$$W^S(M_0) \cap X_0 = \emptyset. \tag{34}$$

Based on the continuity of solutions with respect to the initial conditions, for any $\hat{\epsilon} > 0$, there exists $\delta > 0$ small enough such that for all $(S(0), H(0), E(0), I(0), C(0), R(0)) \in X_0$ with $\|(S(0), H(0), E(0), I(0), C(0), R(0)) - M_0\| \leq \delta$, we have

$$\|u(t, (S(0), H(0), E(0), I(0), C(0), R(0))) - u(t, M_0)\| < \hat{\epsilon}, \qquad \forall t \in [0, \omega]. \tag{35}$$

We claim that

$$\begin{aligned} \limsup_{m\to\infty} &\|P^m(S(0), H(0), E(0), I(0), C(0), R(0)) - M_0\| \\ &\geq \delta, \quad \forall (S(0), H(0), E(0), I(0), C(0), R(0)) \in X_0. \end{aligned} \tag{36}$$

Suppose by contradiction; that is, we suppose $\limsup_{m\to\infty} \|P^m(S(0), H(0), E(0), I(0), C(0), R(0)) - M_0\| < \delta$ for some $(S(0), H(0), E(0), I(0), C(0), R(0)) \in X_0$. Without loss of generality, we assume that $\|P^m(S(0), H(0), E(0), I(0), C(0), R(0)) - M_0\| < \delta, \ \forall m \geq 0$. Thus,

$$\begin{aligned} \|u(t, P^m(S(0), H(0), E(0), I(0), C(0), R(0))) - u(t, M_0)\| < \hat{\epsilon}, \\ \forall t \in [0, \omega] \text{ and } m \geq 0. \end{aligned} \tag{37}$$

Moreover, for any $t \geq 0$, we can write $t = t' + n\omega$ with $t' \in [0, \omega)$ and n being the greatest integer less than or equal to t/ω. Then we obtain

$$\begin{aligned} &\|u(t, (S(0), H(0), E(0), I(0), C(0), R(0))) - u(t, M_0)\| \\ &= \|u(t', P^m(S(0), H(0), E(0), I(0), C(0), R(0))) - u(t', M_0)\| < \hat{\epsilon} \end{aligned} \tag{38}$$

for any $t \geq 0$. Let $\big(S(t), H(t), E(t), I(t), C(t), R(t)\big) = u\big(t, (S(0),\ H(0), E(0), I(0), C(0), R(0))\big)$. It follows that

$$\begin{aligned} \frac{\alpha+\mu}{\alpha+\mu+\phi} - \hat{\epsilon} \quad &< S(t) < \quad \frac{\alpha+\mu}{\alpha+\mu+\phi} + \hat{\epsilon} \\ \frac{\phi}{\alpha+\mu+\phi} - \hat{\epsilon} \quad &< H(t) < \quad \frac{\phi}{\alpha+\mu+\phi} + \hat{\epsilon} \\ 0 \quad &< I(t) < \quad \hat{\epsilon} \\ 0 \quad &< E(t) < \quad \hat{\epsilon} \\ 0 \quad &< C(t) < \quad \hat{\epsilon} \end{aligned}$$

Then,

$$\begin{aligned} \frac{dE}{dt} &= \beta(t)I(t)(S(t) + (1-\epsilon)H(t)) - (\mu+\gamma)E(t) \\ &\geq \beta(t)I(t)\left(\frac{\alpha+\mu}{\alpha+\mu+\phi} - \hat{\epsilon} + (1-\epsilon)(\frac{\phi}{\alpha+\mu+\phi} - \hat{\epsilon})\right) - (\mu+\gamma)E(t) \\ &= \beta(t)I(t)\left(\frac{\alpha+\mu+(1-\epsilon)\phi}{\alpha+\mu+\phi} - \hat{\epsilon}(2-\epsilon)\right) - (\mu+\gamma)E(t) \\ &= -(\mu+\gamma)E(t) + \beta(t)\left(\frac{\alpha+\mu+(1-\epsilon)\phi}{\alpha+\mu+\phi}\right)I(t) - \hat{\epsilon}(2-\epsilon)\beta(t)I(t) \end{aligned}$$

Thus, we obtain,

$$\frac{d}{dt}\begin{bmatrix} E \\ I \end{bmatrix} \geq [F - V - \hat{\epsilon}\cdot K]\cdot\begin{bmatrix} E \\ I \end{bmatrix} \tag{39}$$

where $F - V$ is given by equation (23) and

$$\hat{\epsilon}\cdot K = \hat{\epsilon}\cdot\begin{bmatrix} 0 & (2-\epsilon)\beta(t) \\ 0 & 0 \end{bmatrix} \tag{40}$$

Note that $R_0 > 1$ if and only if $\rho(\Phi_{F-V}(\omega)) > 1$. Thus, for $\hat{\epsilon} > 0$ small enough we have $\rho(\Phi_{F-V-\hat{\epsilon}\cdot K}(\omega)) > 1$. Using Lemma 1 and the comparison principle, we immediately obtain

$$\lim_{t\to\infty} E(t) = \infty \quad \text{and} \quad \lim_{t\to\infty} I(t) = \infty, \tag{41}$$

which is a contradiction.

Hence, M_0 is acyclic in M_∂, and P is uniformly persistent with respect to $(X_0, \partial X_0)$, which implies the uniform persistence of the solutions to the original system [23]. Consequently, the Poincaré map P has a fixed point $(\tilde{S}(0), \tilde{H}(0), \tilde{E}(0), \tilde{I}(0), \tilde{C}(0), \tilde{R}(0)) \in X_0$, and it can be easily seen that $\tilde{S}(0), \tilde{H}(0), \tilde{C}(0), \tilde{R}(0) \neq 0$. Thus, $(\tilde{S}(0), \tilde{H}(0), \tilde{E}(0), \tilde{I}(0), \tilde{C}(0), \tilde{R}(0)) \in (0,1)^6$ and

$$(\tilde{S}(t), \tilde{H}(t), \tilde{E}(t), \tilde{I}(t), \tilde{C}(t), \tilde{R}(t)) = u(t, (\tilde{S}(0), \tilde{H}(0), \tilde{E}(0), \tilde{I}(0), \tilde{C}(0), \tilde{R}(0)))$$

is a positive ω-periodic solution of the system. □

2.5. **Numerical results.** We have conducted numerical simulation for various values of $\beta(t)$ and results show that even though seasonality has been incorporated in FMDV transmission, $\mathcal{R}_0$ remains a sharp threshold for disease dynamics. The disease is eradicated when $\mathcal{R}_0 < 1$ and uniformly persists when $\mathcal{R}_0 > 1$. We illustrate this through several figures. Without loss of generality, we set the phase $\varphi = 0$ in the numerical simulation.

In Figure 3, we plot the value of $\mathcal{R}_0$ when the parameter β_0 varies. As can be easily observed from equations (17) and (19), $\mathcal{R}_0 = \rho(L)$ is directly proportional to β_0. This is analogue to the autonomous result, equation (8), where $\mathcal{R}_e$ is proportional to β. The graph of $\mathcal{R}_0$ vs. β_0 in Figure 3, clearly seen as a straight line starting from the origin, is consistent with the analytic prediction. In particular, we observe that $\mathcal{R}_0 = 1$ when $\beta_0 \approx 0.52$. Thus, whenever the baseline value (or time-average) of $\beta(t)$ is greater than 0.52 per day, FMD persists in the community. Note that this estimate is slightly higher than that from the $\mathcal{R}_e$ result (representing the autonomous, or time-averaged, system) shown in Figure 2, implying that seasonal variation allows a higher threshold baseline value of the transmission rate for FMD outbreaks. In other words, the autonomous system (1) without incorporation of seasonal impacts might overestimate the disease risk.

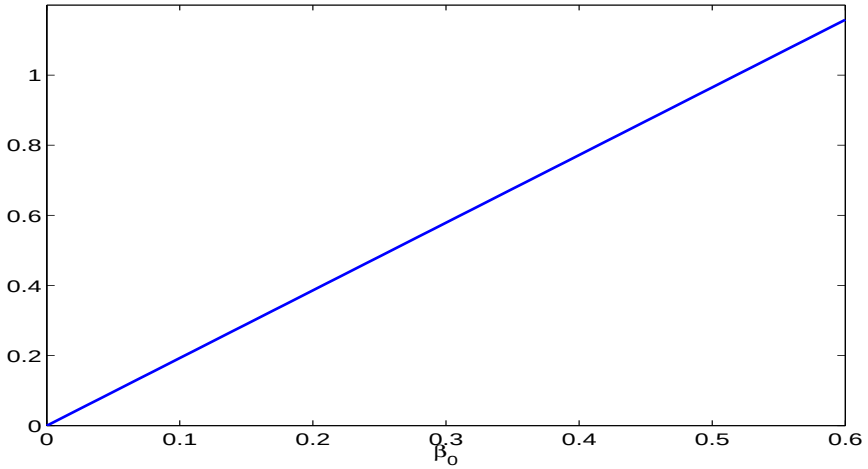

FIGURE 3. Plot of the periodic threshold of $\mathcal{R}_0$ for various β_0. Here $a = 0.5$, and other parameter values are given in Table 1. Note that $\mathcal{R}_0 = 1$ when $\beta_0 \approx 0.52$.

Next, we plot the value of $\mathcal{R}_0$ when the parameter a varies, in Figure 4. We observe that $\mathcal{R}_0$ is decreasing as the value of a increases, indicating that a regular oscillation of the transmission rate about its mean value (here $\beta_0 = 0.6$) could reduce the overall reproduction number. That is, the prediction based on the autonomous (or time-averaged) system could overestimate the disease risk, a result similar to what we concluded from Figure 3. In addition, we note that when $a = 0.5$ in Figure 4, $\mathcal{R}_0$ is approximately 1.16, which is consistent with the result (when $\beta_0 = 0.6$) shown in Figure 3.

Numerical results in Figures 5 and 6 show typical infection curves when $\mathcal{R}_0 < 1$ and $\mathcal{R}_0 > 1$, respectively. When $\mathcal{R}_0 < 1$, the disease quickly dies out and the

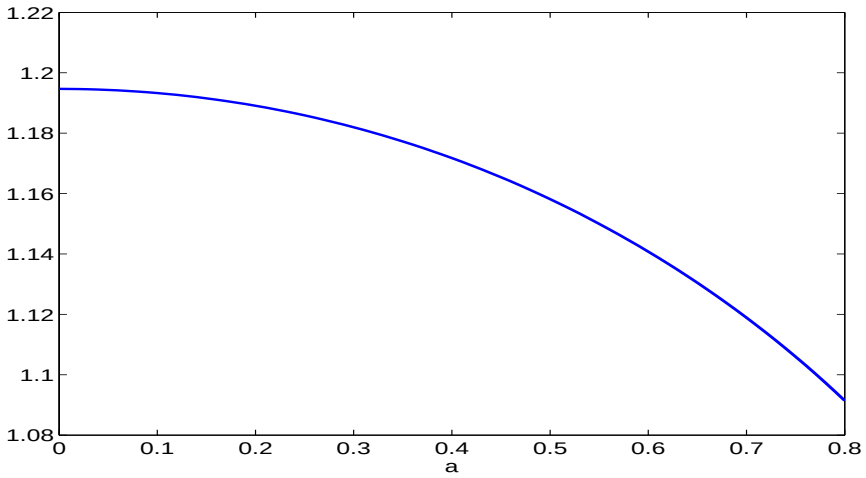

FIGURE 4. Plot of the periodic threshold of $\mathcal{R}_0$ for various a. Here $\beta_0 = 0.6$, and other parameter values are given in Table 1.

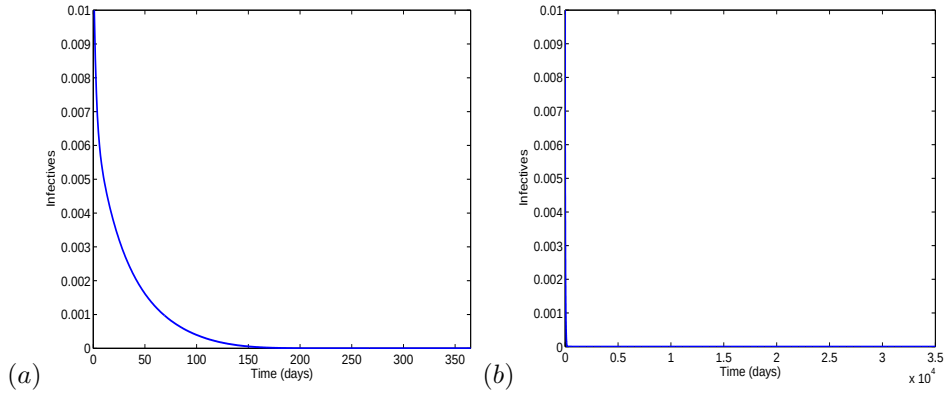

FIGURE 5. (a) An infection curve when $\mathcal{R}_0 < 1$ with initial condition $I(0) = 0.01$. (b) Long-term behavior of the infection curve. The solution quickly converges to the FMD-free equilibrium with $I^0 = 0$.

FMD-free equilibrium is asymptotically stable further evidenced by the long-term behavior shown in Figure 5(b). On the other hand, when $\mathcal{R}_0 > 1$, the disease persists, and following a transient period, the infection approaches an ω-periodic solution. Figure 6(b) zooms in to highlight the periodic solution observed after the transient period.

3. **Concluding remarks.** In this paper, two mathematical models for FMD have been proposed. The first model is an autonomous system with constant parameters that incorporates the relevant biological components and FMD vaccination. The effective reproductive number $\mathcal{R}_e$ was derived and proven to be a sharp threshold for disease dynamics. Particularly, when $\mathcal{R}_e > 1$, there exists a unique endemic equilibrium that is locally asymptotically stable. Numerical results provided evidence

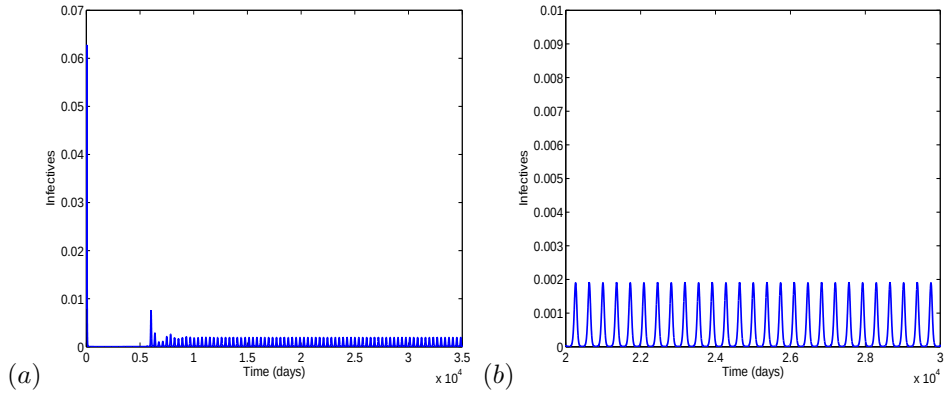

FIGURE 6. (*a*) An infection curve when $\mathcal{R}_0 > 1$ with initial condition $I(0) = 0.01$. (*b*) Zoomed in to ω-periodic solution after a transient period.

that vaccination alone may not be sufficient to eradicate FMD in the community when the disease transmission rate is sufficiently high, though the vaccine may have a positive effect on lowering the disease risks and reducing cumulative FMD cases when an outbreak occurs.

In the second model, we extended the autonomous system to a periodic environment to analyze the impacts of seasonal variation that may affect the movements of animals and, consequently, FMDV transmission. The basic reproduction number $\mathcal{R}_0$ was derived and and our analysis showed that $\mathcal{R}_0$ remains a sharp threshold for disease dynamics even in a periodic environment. Thus, if $\mathcal{R}_0 < 1$, FMD will be eradicated. Further, we proved uniform persistence of the disease as well as the existence of a nontrivial periodic solution when $\mathcal{R}_0 > 1$. Investigating the persistence of the disease with oscillating reoccurrence of infection spreading can lead to greater insights into FMD dynamics and avenues for establishing effective and optimal control strategies as well as curtailing any financial losses to the farming industry.

Although in the second model we have focused on the periodic oscillation of the transmission rate, β, similar extensions can be made to other model parameters to investigate the effects of their seasonal variation on FMD dynamics. The analysis of disease extinction and persistence can be conducted in the same way. Fitting those key model parameters with realistic seasonal data will improve our model and its applicability.

Appendix. We list the following standard result based on the center manifold theory [3], which we use to prove Theorem 2.3.

Theorem 3.1. *Consider the following general system of ordinary differential equations with a parameter* ϕ,

$$\frac{dx}{dt} = f(x, \phi), f : \mathbb{R}^n \times \mathbb{R} \to \mathbb{R}^n \text{and } f \in \mathbb{C}^2(\mathbb{R}^n \times \mathbb{R}). \tag{42}$$

Without loss of generality, it is assumed that 0 is an equilibrium for system (42) for all values of the parameter ϕ*; that is,* $f(0, \phi) = 0$ *for all* ϕ*. Assume*

(A1): $A = D_x f(0,0) = \left(\frac{\partial f_i}{\partial x_j}(0,0)\right)$ *is the linearisation of system (42) around the equilibrium* 0 *with* ϕ *evaluated at* 0. *Zero is a simple eigenvalue of* A *and other eigenvalues of* A *have negative real parts;*

(A2): *Matrix* A *has a right eigenvector* w *and a left eigenvector* v *corresponding to the zero eigenvalue.*

Let f_k *be the* k*th component of* f *and*

$$\begin{aligned} a &= \sum_{k,i,j=1}^{n} v_k w_i w_j \frac{\partial^2 f_k}{\partial x_i \partial x_j}(0,0), \\ b &= \sum_{k,i=1}^{n} v_k w_i \frac{\partial^2 f_k}{\partial x_i \partial \phi}(0,0). \end{aligned} \tag{43}$$

The local dynamics of (42) around 0 *are governed by* a *and* b *in the following manner:*

(i): $a > 0, b > 0$. *When* $\phi < 0$ *with* $|\phi| \ll 1$, 0 *is locally asymptotically stable, and there exists a positive unstable equilibrium; when* $0 < \phi \ll 1$, 0 *is unstable and there exists a negative and locally asymptotically stable equilibrium;*

(ii): $a < 0, b < 0$. *When* $\phi < 0$ *with* $|\phi| \ll 1$, 0 *is unstable; when* $0 < \phi \ll 1$, *0 is locally asymptotically stable, and there exists a positive unstable equilibrium;*

(iii): $a > 0, b < 0$. *When* $\phi < 0$ *with* $|\phi| \ll 1$, 0 *is unstable, and there exists a locally asymptotically stable negative equilibrium; when* $0 < \phi \ll 1$, 0 *is stable, and a positive unstable equilibrium appears;*

(iv): $a < 0, b > 0$. *When* ϕ *changes from negative to positive,* 0 *changes its stability from stable to unstable. Correspondingly, a negative equilibrium becomes positive and locally asymptotically stable.*

Acknowledgments. The work of JW is partially supported by the National Science Foundation under Grant Numbers 1412826 and 1557739. The authors are grateful to the two anonymous reviewers for their comments to improve this paper.

REFERENCES

[1] F. Aftosa, *Foot and Mouth Disease*, http://www.cfsph.iastate.edu/Factsheets/pdfs/foot_and_mouth_disease.pdf, (Accessed September 2014)

[2] A. Alexandersen, Z. Zhang and I. A. Donaldson, Aspects of the persistence of foot-and -mouth disease virus in animals-the carrier problem, *Microbes and Infection*, **4** (2002), 1099–1110.

[3] C. Castillo-Chavez and B. Song, Dynamical models of tuberculosis and their applications, *Mathematical Biosciences and Engineering*, **1** (2004), 361–404.

[4] M. E. Chase-Topping, I. Handel, B. M. Bankowski, N. D. Juleff, D. Gibson, S. J. Cox, M. A. Windsor, E. Reid, C. Doel, R. Howey, P. V. Barnett, M. E. J. Woolhouse and B. Charleston, Understanding foot-and-mouth disease virus transmission biology: Identification of the indicators of infectiousness, *Veterinary Research*, **44** (2013), p46.

[5] T. A. Dekker, H. Vernooij, A. Bouma and A. Stegeman, Rate of foot-and-mouth disease virus transmission by carriers quantified from experimental data, *Risk Analysis*, **28** (2008), 303–309.

[6] O. Diekmann and J. Heesterbeek, *Mathematical Epidemiology of Infectious Diseases: Model Building, Analysis and Interpretation*, Wiley, 2000.

[7] J. Gloster, H. Champion, J. Sorensen, T. Mikkelsen, D. Ryall, P. Astrup, S. Alexandersen and A. Donaldson, Airborne transmission of foot-and-mouth disease virus from Burnside Farm, Heddon-on-the-Wall, Northumberland, during the 2001 epidemic in the United Kingdom, *The Veterinary Record*, **152** (2003), 525–533.

[8] R. R. Kao, L. Danon, D. M. Green and I. Z. Kiss, Demographic structure and pathogen dynamics on the network of livestock movements in Great Britain, *Proceedings of the Royal Society B*, **273** (2006), 1999–2007.
[9] M. J. Keeling, M. E. J. Woolhouse, R. M. May, G. Davies and B. T. Grenfell, Modelling vaccination strategies against foot-and-mouth disease, *Nature*, **421** (2003), 136–142.
[10] R. P. Kitching, Identification of foot and mouth disease virus carrier and subclinically infected animals and differentiation from vaccinated animals, *Revue scientifique et technique (International Office of Epizootics)*, **21** (2002), 531–538.
[11] R. P. Kitching, A. M. Humber and M. V. Thrusfield, A review of foot-and-mouth disease with special consideration for the clinical and epidemiological factors relevant to predictive modelling of the disease, *Veterinary Journal*, **169** (2005), 197–209.
[12] T. J. Knight-Jones, A. N. Bulut, K. D. Stark, D. U. Pfeiffer, K. J. Sumption and D. J. Paton, Retrospective evaluation of foot-and-mouth disease vaccine effectiveness in Turkey, *Vaccine*, **32** (2014), 1848–1855.
[13] G. E. Lahodny Jr., R. Gautam and R. Ivanek, Estimating the probability of an extinction or major outbreak for an environmentally transmitted infectious disease, *Journal of Biological Dynamics*, **9** (2015), 128–155.
[14] J. S. LaSalle, *The stability of Dynamical Systems*, SIAM: Philadelphia, 1976.
[15] S. Mushayabasa, C. P. Bhunu and M. Dhlamini, Impact of vaccination and culling on controlling foot and mouth disease: a mathematical modeling approach, *World Journal of Vaccines*, **1** (2011), 156–161.
[16] S. Parida, Vaccination against foot-and-mouth disease virus: Strategies and effectiveness, *Expert Review of Vaccines*, **8** (2009), 347–365.
[17] D. Posny and J. Wang, Modelling cholera in periodic environments, *Journal of Biological Dynamics*, **8** (2014), 1–19.
[18] D. Posny and J. Wang, Computing basic reproductive numbers for epidemiological models in nonhomogeneous environments, *Applied Mathematics and Computation*, **242** (2014), 473–490.
[19] N. Ringa and C. T. Bauch, Impacts of constrained culling and vaccination on control of foot and mouth disease in near-endemic settings: A pair approximation model, *Epidemics*, **9** (2014), 18–30.
[20] Y. Sinkala, M. Simuunza, J. B. Muma, D. U. Pfeiffer, C. J. Kasanga and A. Mweene, Foot and mouth disease in Zambia: Spatial and temporal distributions of outbreaks, assessment of clusters and implications for control, *Onderstepoort Journal of Veterinary Research*, **81** (2014), 6pp.
[21] P. Van den Driessche and J. Watmough, Reproduction numbers and sub-threshold endemic equilibria for compartmental models of disease transmission, *Mathematical Biosciences*, **180** (2002), 29–48.
[22] W. Wang and X. Zhao, Threshold dynamics for compartmental epidemic models in periodic environments, *Journal of Dynamics and Differential Equations*, **20** (2008), 699–717.
[23] X.-Q. Zhao, *Dynamical Systems in Population Biology*, Springer-Verlag, New York, 2003.

Received April 08, 2015; Accepted November 03, 2015.

E-mail address: steadymushaya@gmail.com
E-mail address: drew.posny@ars.usda.gov
E-mail address: Jin-Wang02@utc.edu